ELSEVIER

Chemical Engineering Science 58 (2003) 5087–5102

Chemical Engineering Science

www.elsevier.com/locate/ces

A simulation of oscillatory behavior in the NO + H_2 reaction on Pt(100): effect of diffusion and blocking sites

Francisco Vidal Caballero[a], Luis Vicente[b,*]

[a] *Tecnológico de Estudios Superiores de Ecatepec, Av. Hank González s/n, Col. Valle de Anáhuac Ecatepec de Morelos, 55210, Mexico*
[b] *Departamento de Física y Química Teórica, Facultad de Química, UNAM, 04510 México, D. F., Mexico*

Received 4 November 2002; received in revised form 18 July 2003; accepted 12 August 2003

Abstract

The catalytic reduction of nitric oxide by H_2 over the Pt(100) surface is studied as a function of partial pressures of the reactants. The mathematical mean field model, originally proposed by Makeev and Nieuwenhuys (J. Chem. Phys. 108 (1998a) 3740) shows kinetic oscillations of the reaction products and near the critical point the dependence of the amplitude of oscillations on the partial pressures ratio p is shown to be very close to that predicted for the Hopf supercritical bifurcation. The model has been extended to include the effect of blocking sites (poisoning) on the catalyst surface. This effect changes the period of the oscillations. Diffusion of the adspecies NO has also been studied and we show in what way it modifies the nonlinear behavior of the kinetic oscillations and the transition to chaos through period-doubling bifurcations. The influence of defects on global coupling as they are increased continuously is also studied. Finally, we use Monte Carlo simulations to show the species distributions and growth as they oscillate in time.

Keywords: Adsorption; Kinetics; Mathematical; Modelling; Nonlinear dynamics; Monte Carlo simulation

1. Introduction

The catalytic reduction of NO with either CO or H_2 is very important due to the contaminant effects of NO in air (Egelhoff, 1982). In general, heterogeneous catalysis of different adsorbates as CO + O_2, CO + NO, NO + H_2, NO + NH_3 on low index Pt single crystal surfaces show complex dynamical behavior as oscillations, pattern formation and chaotic behavior. This in effect has been reviewed by Imbihl (1993), Slinko and Jaeger (1994) and Imbihl and Ertl (1995).

In particular, the catalytic reduction of nitric oxide by hydrogen over the Pt(100) surface has been the subject of both experimental and theoretical studies. Among the properties studied there is the so-called "surface explosion" (Lesley and Schmidt, 1985) where the coadsorbed NO and H_2 react to form extremely narrow product peaks observed in temperature-programmed reaction experiments. Another very interesting property is the occurrence of kinetic oscillations. These kinetic oscillations were found to occur for gas reactant pressures in the range 10^{-6}–10^{-5} mbar in the range of temperatures from 430 to 500 K (Siera et al., 1991; Madden and Imbihl, 1991; Cobden et al., 1992).

When there is adsorption of atoms in a surface their presence affects the position of the topmost substrate atoms and at a certain coverage the surface may undergo a phase transition (SPT). An important feature of the system Pt(100) is that the clean surface undergoes a "hex"-reconstruction, but significant local coverage of CO or NO lift this hex-reconstruction to recover a 1 × 1-structure. If the coverage of NO adsorbed on the 1 × 1 patches drop below its critical value the surface transforms into the hex phase again. Madden and Imbihl (1991) demonstrated that the complex dynamical behavior shown by the NO + H_2 reaction on Pt(100) arises as a consequence of the 1 × 1 → hex phase transition and of the coexistence of multiple reaction channels in which either N_2 and H_2O or NH_3 appear as reaction products.

To describe the occurrence of kinetic oscillations Lombardo et al. (1993) proposed a model consisting of seven ordinary differential equations for describing the coverage changes of six adsorbed species ($NO^{1\times1}$, NO^{hex}, $NH_3^{1\times1}$, $H^{1\times1}$, $N^{1\times1}$, $O^{1\times1}$), as well as

* Corresponding author. Tel.: +52-55-5665-0819; fax: +52-55-5622-3719.
E-mail address: vicente@eros.pquim.unam.mx (L. Vicente).

0009-2509/$ - see front matter © 2003 Elsevier Ltd. All rights reserved.
doi:10.1016/j.ces.2003.08.013

an equation for the $1 \times 1 \rightarrow$ hex phase transformation. Gruyters et al. (1996) proposed a new model based on a strongly non-linear power law for the $(1 \times 1) - NO$ island growth rate from the hex phase with an apparent reaction order in the local NO coverage on the hex phase. Cobden et al. (1992) proposed a different mechanism to explain the kinetic oscillations. They used a "vacancy model" in which the oscillations are due to autocatalytic surface reaction, which increase the number of vacant sites for NO dissociation. Makeev and Nieuwenhuys (1998a) have developed a mathematical model to prove that autocatalysis of NO decomposition by vacant sites is one of the main properties that keep the system oscillating. The other major ingredient is the coverage dependency of the activation energies for NO and CO desorption. In fact, the catalytic reduction of NO by CO over Pt(100) exhibit a very similar dynamic behavior and in this system Fink et al. (1991b) have shown that oscillatory behavior occurs in two windows. In the low temperature window (around 400 K) the system presents oscillatory behavior without involvement of the surface structural transformation and in the upper temperature window (around 450 K)there is a coupling with surface phase transition between the 1×1 and hex phase. Similarly, the $NO + H_2/Pt(100)$ system at relatively low temperatures, oscillations take place on a surface that is completely in the 1×1 structure. In fact, Makeev and Nieuwenhuys (1998a) have shown that the $1 \times 1 \rightleftharpoons$ hex is not essential for producing oscillatory behaviour in the low temperature window.

Most of the theoretical studies concerning catalytic oxidations or reduction on Pt assumed that adsorption and reaction takes place on a substrate of pure metal without any defects or impurities. However, it is not possible to remove all impurities in a real crystal sample. On the contrary, sometimes some foreign atoms can be intentionally deposited on a given substrate to form a composite catalyst for special use. The impurities decrease the number of available adsorption sites on the surface and can thus be considered as blocking sites. For example, Asakura et al. (1994, 1997) have shown that active reaction–diffusion media can be constructed containing inert (passive or active) inclusions and that the scale and nature of these inclusions can drastically affect spontaneous pattern formation on the modified substrate.

The most familiar description of heterogeneous catalytic reactions is the mean field approximation (MF) in the reaction kinetics. Their validity is however limited since it does not take into account the occurrence of stochastic fluctuations (Peeters et al., 1990) and correlations. Among the attempts to built more microscopic models Monte Carlo (MC) simulations applied to surface reactions should be mentioned. They have shown a great success since the work of Ziff et al. (1986) on an irreversible monomer–dimer reaction mimicking by example the CO oxidation on a metal surface. A recent review of these simulations can be found in the work by Zhdanov (2002). These simulations incorporate the discreteness of the reactive events in an intrinsic manner and are thus complementary of the MF studies.

In this paper we make an study of the $NO + H_2/Pt(100)$ reaction. First, we use the MF approach to study the low temperature window and consequently do not consider the $(1 \times 1) \rightarrow$ hex SPT. We use the mathematical model proposed by Makeev and Nieuwenhuys (1998a) which reproduces very well the experimental observations of surface explosion, temperature programmed desorption spectra and regular and chaotic oscillations of the $NO + H_2/Pt$ system. This model is presented in Section 2. In Section 2.1 we extend the model to include the effect of impurities (blocking sites) on the oscillations. In Section 3 we consider a nonuniform surface both in one and two-dimensions. This allows considering spatial patterns through the inclusion of diffusion of one of the reactants and the influence of defects. The defects are considered here as sites with different sticking coefficients.

Second, in Section 4 we make Monte Carlo simulations, which show the coverage distributions on time and complements the MF calculations. Finally, Section 5 contains our conclusions.

2. Model in an uniform surface

The following set of elementary step have been formulated by Makeev and Nieuwenhuys (1998a):

$$NO(g) + * \underset{k_2}{\overset{k_1}{\rightleftharpoons}} NO_{ads}, \qquad \text{(R1–R2)}$$

$$H_2(g) + 2* \underset{k_4}{\overset{k_3}{\rightleftharpoons}} 2H_{ads}, \qquad \text{(R3–R4)}$$

$$NO_{ads} + * \underset{k_6}{\overset{k_5}{\rightleftharpoons}} N_{ads} + O_{ads}, \qquad \text{(R5–R6)}$$

$$2N_{ads} \overset{k_7}{\rightarrow} N_2(g) + 2^*, \qquad \text{(R7)}$$

$$O_{ads} + H_{ads} \overset{k_8}{\rightarrow} OH_{ads} + *, \qquad \text{(R8)}$$

$$N_{ads} + H_{ads} \underset{k_{10}}{\overset{k_9}{\rightleftharpoons}} NH_{ads} + *, \qquad \text{(R9–R10)}$$

$$NH_{ads} + H_{ads} \overset{k_{11}}{\rightarrow} NH_{2ads} + *, \qquad \text{(R11)}$$

$$NH_{3ads} \overset{k_{12}}{\rightarrow} NH_3(g) + *, \qquad \text{(R12)}$$

$$NH_{2ads} + H_{ads} \xrightarrow{k_{13}} NH_{3ads} + *, \quad \text{(R13)}$$

$$OH_{ads} + H_{ads} \xrightarrow{k_{14}} H_2O_{ads} + *, \quad \text{(R14)}$$

$$H_2O_{ads} \xrightarrow{k_{15}} H_2O(g) + *, \quad \text{(R15)}$$

where * denotes a free adsorption site of the Pt(100)-(1×1) surface; $NO(g), H_2(g)$ are the reactants in the gas-phase with partial pressures p_{NO} and p_{H_2}, respectively. The reaction products are $N_2(g), NH_3(g)$ and $H_2O(g)$. Adsorbed species are denoted by $(NO)_{ads}, (H)_{ads}, (N)_{ads}, (O)_{ads}, (NH)_{ads}$, and $(NH_3)_{ads}$.

This reaction mechanism includes adsorption/desorption of NO and H_2 (steps 1, 2 with rate constants k_i), reversible dissociation of $(NO)_{ads}$ (step 3), dinitrogen formation (step 4), ammonia formation (steps 6–9) via intermediates $(NH)_{ads}$ and $(NH_2)_{ads}$ and water formation (steps 5,10–11) via $(OH)_{ads}$ intermediate. Besides, the desorption of $(H_2O)_{ads}$ and the hydrogenation of intermediates $(OH)_{ads}$ and $(NH_2)_{ads}$ are assumed to be fast processes. In this way only six species are considered (surface coverages are denoted by θ_p, $p = NO, H, N, O, NH, NH_3$). Furthermore the non-ideality of the adsorbed layer is taken into account through lateral interactions ε_{ap}. This quantity reflects microscopically the influence of the local environment on the activation energies of the elementary reaction steps and can be considered as the difference of the lateral interactions in the activated and ground states.

The temporal variation of surface coverages are then described by the following coupled ordinary differential equations (ODEs):

$$\frac{d\theta_{NO}(t)}{dt} = R_1 - R_2 - R_5 + R_6, \quad (1)$$

$$\frac{d\theta_{H}(t)}{dt} = 2R_3 - 2R_4 - 2R_8 - R_9 + R_{10} - 2R_{11}, \quad (2)$$

$$\frac{d\theta_{N}(t)}{dt} = R_5 - 2R_7 - R_6 - R_9 + R_{10}, \quad (3)$$

$$\frac{d\theta_{O}(t)}{dt} = R_5 - R_6 - R_8, \quad (4)$$

$$\frac{d\theta_{NH}(t)}{dt} = R_9 - R_{10} - R_{11}, \quad (5)$$

$$\frac{d\theta_{NH_3}(t)}{dt} = R_{11} - R_{12}. \quad (6)$$

R_i are the rate of the elementary steps ($R1$–$R12$) given above:

$$R_1 = k_1 p_{NO} S_{NO} \theta_*, \quad R_2 = k_2 \theta_{NO} I_2,$$

$$R_3 = k_2 p_{H_2} s_{H_2} (\theta_*)^2, \quad R_4 = k_4 (\theta_H)^2 I_4,$$

$$R_5 = k_5 \theta_{NO} \theta_* I_5, \quad R_6 = k_6 \theta_N \theta_O,$$

$$R_7 = k_7 (\theta_N)^2 I_7,$$

$$R_8 = k_8 \theta_O \theta_H,$$

$$R_9 = k_9 \theta_N \theta_H, \quad R_{10} = k_{10} \theta_{NH} \theta_*,$$

$$R_{11} = k_{11} \theta_{NH} \theta_H,$$

$$R_{12} = k_{12} \theta_{NH_3},$$

where

$$\theta_* = 1 - \theta_{NO} - \theta_H - \theta_N - \theta_O - \theta_{NH} - \theta_{NH_3} - \theta_d$$

$$k_\alpha = \nu_\alpha \exp[-E_\alpha/(RT)], \alpha = 1, \ldots, 12,$$

$$I_\alpha = \left(\theta_* + \sum_{p=1}^{6} \theta_p \exp[\varepsilon_{\alpha p}/(RT)] \right)^{m_\alpha},$$

θ_* the fraction of empty sites, θ_d the fraction of blocked sites, m_α the number of nearest-neighbor sites, S_i the sticking coefficient.

The factor I_α takes into account the influence of lateral interactions in the framework of the lattice-gas model for a well-mixed adlayer. When there is no such lateral interactions $\varepsilon_{\alpha p} = 0$ and $I_\alpha = 1$. The kinetic parameters given in Table 1 where taken from surface science studies by Fink et al. (1991a), Dixon-Warren et al. (1995) and Makeev and Nieuwenhuys (1998a). The parameters for lateral interactions were taken from this last reference and are $|\varepsilon_{\alpha,i}| < 2$. The model Eqs. (1)–(6) are strongly stiff and have to be integrated with an adequate numerical procedure. We used Gear's method (1971) for solving stiff ODEs, which provides efficiency and accuracy of integration.

Table 1
The energy and bare frequency parameters that enter the expression for the various rate constants $k = \nu \exp(-E/RT)$

Reaction step, α	$\nu_\alpha(s^{-1})$	E_α(kcal/mol)
1	2.14×10^5 mbar^{-1}	0
2	1.7×10^{15} mbar^{-1}	37
3	8.28×10^5 mbar^{-1}	0
4	10^{12}	25
5	2×10^{15}	28
6	2×10^{15}	23
7	10^{13}	24
8	10^{13}	13
9	10^{9}	15
10	10^{13}	29
11	10^{9}	17.7
12	10^{9}	19

$S_{NO}k_1 = 1.93 \times 10^5$(mbar^{-1} s^{-1}), $S_{H_2}k_3 = 1.656 \times 10^5$(mbar^{-1} s^{-1}).

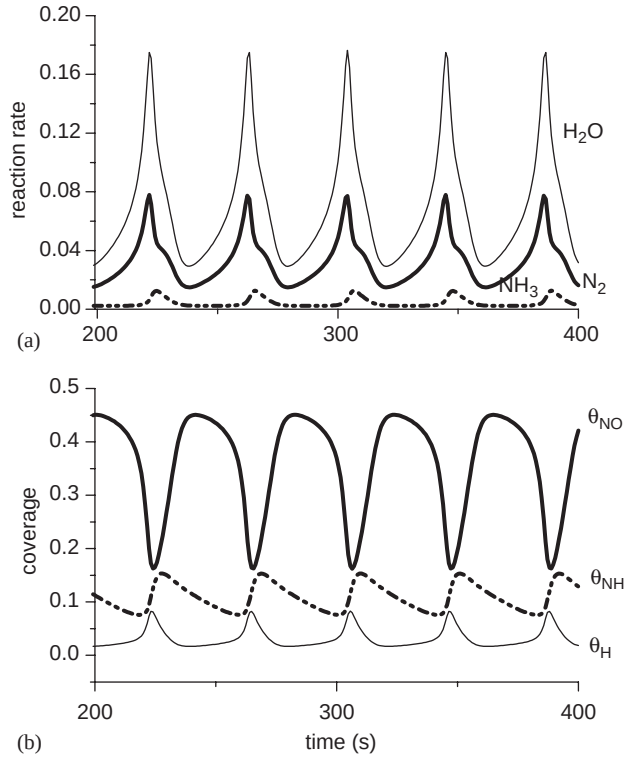

Fig. 1. (a) H_2O, NH_3, N_2 production rates vs time for $T = 434$ K, $p_{NO} = 1.1 \times 10^{-6}$ mbar and $p_{H_2} = 7.6 \times 10^{-6}$ mbar; (b) absorbate coverages of NO, NH and H.

2.1. Sustained oscillations and chaos: effect of poisoning

If the gas pressures are fixed, self-sustained oscillations can be observed for certain temperatures. For example, Fig. 1b shows oscillations in the coverages θ_{NO}, θ_{NH} and θ_H with $T = 434$ K, $p_{NO} = 1.1 \times 10^{-6}$ mbar and $p_{H_2} = 7.6 \times 10^{-6}$ mbar. The oscillation period is around 42 s which is very similar to that found experimentally. When θ_{NO} is at a maximum there is low catalytic activity (Fig. 1a shows the reaction rates for H_2O, N_2 and NH_3), the reaction is inhibited because the high adsorbate coverage. Then the NO adlayer reacts and there is an autocatalytic increase in the number of vacant sites causing increases in the production rates, θ_{NO} decreases and the other coverages increase. Finally θ_{NO} begins to increase again and the reaction moves back into the low activity state.

Slinko et al. (1992), showed the dependence of the oscillation period, t_{osc}, upon the temperature. They found that t_{osc} increases significantly with decreasing temperature. Cobden et al. (1992) observed a transition from periodic to aperiodic oscillations when the H_2 partial pressure was lowered. The transition to aperiodicity occurs via the Feigenbaum scenario, that is, period-doublings, although period-3 and period-5 oscillations were also found. The (very small) region where complex and chaotic oscillations exist is located at the higher border of the temperature range for oscillations.

Table 2
Intervals of p where different oscillations are found

Oscillatory period	p, mean field	p with diffusion
1-period	2.565–10.27	2.574–10.0
2-period	2.516–2.564	2.522–2.573
4-period	2.5119–2.515	2.518–2.521
8-period	2.5111–2.5118	2.515–2.517
Chaos	2.5011–2.511	2.512–2.514

The case with diffusion refers to $D = 3.85$. See text.

To study this transition in our simulations we change the governing parameter $p = p_{H_2}/p_{NO}$ and all the calculations were performed at $T = 457$ K. Table 2 shows the p intervals where different oscillations can be found. Fig. 2a–e (left column) shows some time series for decreasing values of p. Period-1 (P1) oscillations are shown for $p = 2.58$; period-2 (P2) oscillations for $p = 2.54$; period-4 (P4) oscillations for $p = 2.513$, period-8 (P8) oscillations for $p = 2.5118$. Chaos is developed for $p = 2.511$. Additional information concerning the doubling period to chaos can be obtained by plotting the phase portrait (projection onto the (θ_{NH}, θ_{NO} plane)(Fig. 2a–e, right column). Periodic attractors form closed curves: for the period-n responses closed circuits with n loops emerge. The aperiodic oscillations show a large number of circuits. One important observation is that within this temperature the oscillations are modulated: they are not regular but show in all cases a modulation reflecting the presence of another frequency. A bifurcation diagram for this model was calculated by Makeev and Nieuwenhuys (1998a) revealing the period-doubling route to chaos and an approximate structure of the periodic-chaotic windows. In this diagram periodic and chaotic windows are encountered as p is varied. Indeed, changing the parameter p kinetic oscillations described by ordinary differential equations arise usually via the Hopf supercritical bifurcation (Scott, 1991). According to this scenario the amplitude of oscillations near the critical point is proportional to $(p - p^{cr})^{1/2}$. An analysis of our calculations (Fig. 3) shows that this is the case, the amplitude of oscillations of NO coverage is proportional to $(p_{NO} - p_{NO}^{cr})^x$ with $x = 0.488 \pm 0.013$, a result which is acceptable for that predicted for the Hopf bifurcation.

Now we consider the effect of blocking sites. As was mentioned before, the fact of having a fraction θ_d of available sites blocked (as can be the case of poisoning) can reduce the region of oscillatory behavior as has been shown by Chávez et al. (2000) for the $CO+O_2$ reaction. Fig. 4 shows the effect of increasing θ_d when P8 oscillations are set (Fig. 2d). As can be seen a very small fraction ($\theta_d = 0.00002$) turns the P8 oscillations into P4. Increasing this fraction to $\theta_d = 0.00195$ turns the oscillations into a P2 oscillations and finally increasing to $\theta_d = 0.01$ turns the oscillations into a P1. A further

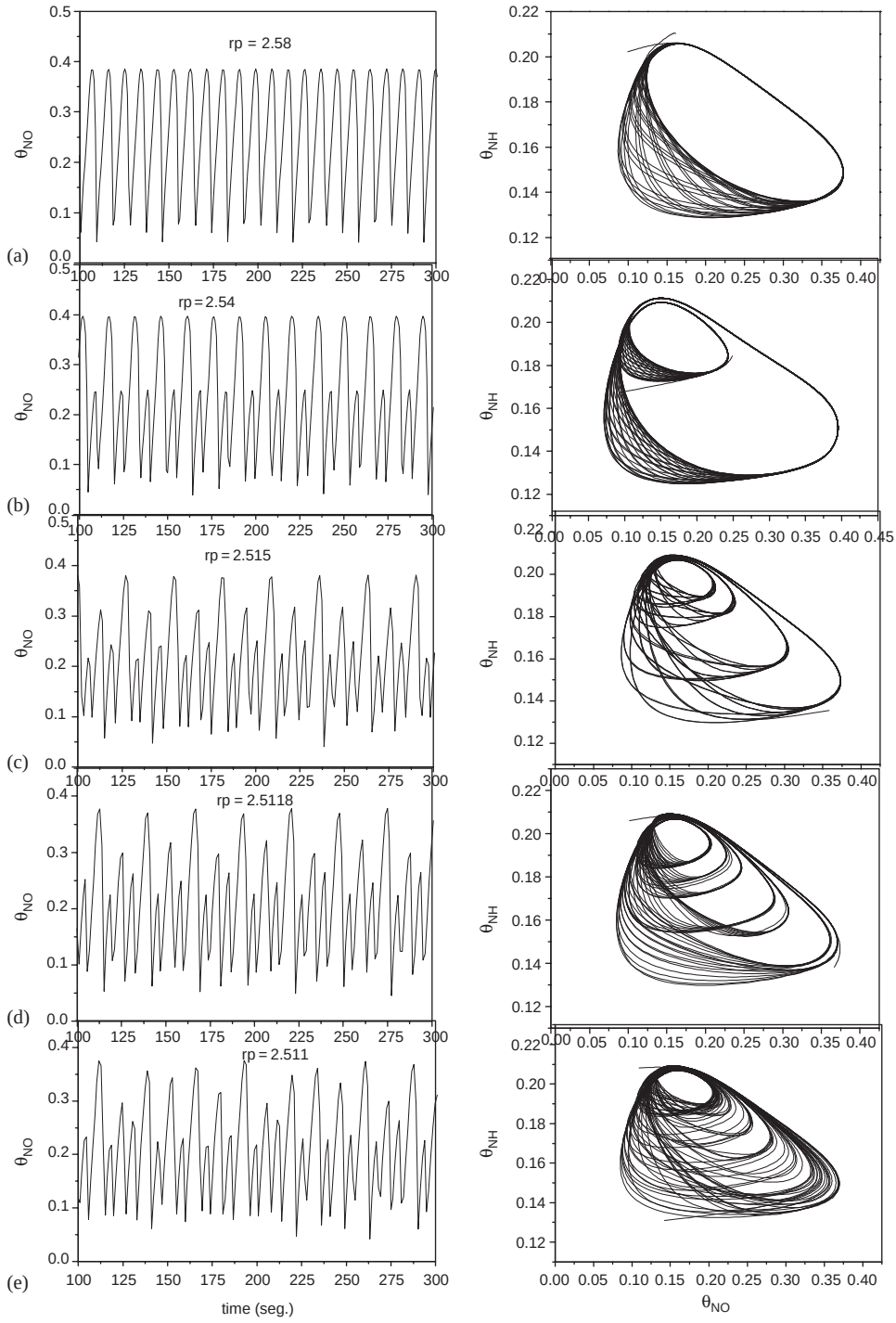

Fig. 2. Period-doubling route to chaos in the NO coverages as a function of time for different values of the pressure ratio $p = p_{H_2}/p_{NO}$: (a) period-1, (b) period-2, (c) period-4, (d) period-8, (e) chaos. The right colums are the corresponding phase portraits θ_{NH} vs θ_{NO}.

increases of the impurity fraction to $\theta_d = 0.0886$ causes the period to lengthen (Fig. 4e) and for larger values the oscillations disappear and a non-oscillatory steady state is reached. If now T or P is changed, the oscillations change again. In the last example by changing p back to $p = 1.8$ P2 oscillations are recovered. The existence range (p, T) for oscillations is now extended to (p, T, θ_d). Thus the model presented here is very sensitive to the number of active available sites for catalytic reactions as the blocked fraction that turned off the oscillations is very low. This is mainly because the autocatalyis of NO decomposition by vacant sites is the main mechanism that keeps the system oscillating. We think that the θ_d

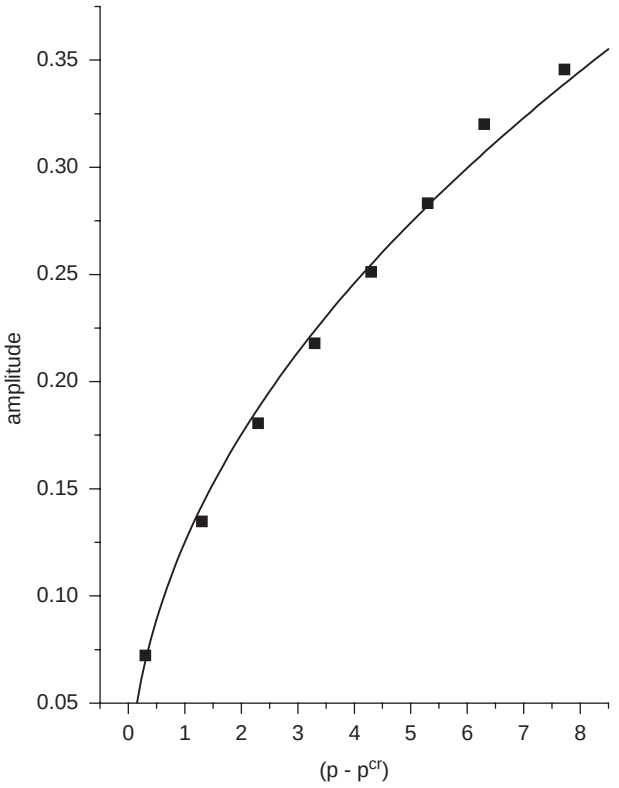

Fig. 3. Amplitude of period-1 oscillations of NO coverage as a function of p. Filled squares denotes the simulations and the solid line corresponds to amplitud $\sim (p - p^{cr})^x$, with $x = 0.488 \pm 0.013$.

fraction must be specific for each reaction and lattice but to our knowledge this has not been verified experimentally. For the simplier reaction $CO + O_2/Pt(100)$ we have shown analytically and by MC simulations (Chávez et al., 2000) that a fraction $\theta_d = 0.6$ of impurities kill completely all oscillations. This value is close to the percolation threshold for a square lattice.

To finish with this section we want to comment about the influence of including a surface reconstruction. As was mentioned above, at relatively large temperatures, oscillations take place on a largely hex-reconstructed surface. Makeev and Nieuwenhuys (1998b) considered the problem by adding to the original mechanism the irreversible migration of *NO* from the hex phase onto the 1×1 phase (trapping) and the equation for the surface phase reconstruction developed by Fink et al. (1991b) and Lombardo et al. (1993). According to this the driving force for the lifting of the hex reconstruction by adsorbed particles is the higher binding energy on the 1×1 phase as compared with the hex phase. After nucleation the adsorbed particles are trapped on the 1×1 regions and these islands grow in size while maintaining a constant local coverage. If the coverage falls below this critical value, the inverse transitions 1×1 is realized.

Makeev and Nieuwenhuys (1998b) found that the oscillations found in this way are very similar with those reported in Section 2.1. They concluded that the $1 \times 1 \rightleftharpoons$ hex SPT of Pt(100) is not essential for producing oscillations, in spite that the oscillations take place on a hex-reconstructed surface at the high temperature window.

3. Nonuniform surface

3.1. One dimension

Investigations of spatial structure formation in heterogeneous catalytic systems have been inspired by the observation of a large variety of patterns on the catalyst surface during single crystal surface studies (Imbihl and Ertl, 1995). In order to consider spatial structures diffusion terms have to be included in the model presented before. In a reaction–diffusion system, the concentrations C_i of the chemical species are described by the following partial differential equation (PDE)

$$\frac{\partial C_i}{\partial t} = f(..C_j,..) + D_i \bigtriangledown^2 C_i,$$

where D_i is the diffusion coefficient for the ith substance and f_i specifies the reaction mechanism. As a first approximation we could consider only NO migration and take $D = 10^{-7}$ m^2/s which is the value proposed by Imbihl et al. (1985, 1986) for CO migration on Pt. This because CO and NO have very similar behavior on Pt(100) (Fink et al., 1991a, b). This value is high as compared to the corresponding D value for H, N and O (Makeev et al., 2001). Mean-field reaction–diffusion equations treat diffusion of distinct adspecies as independent. They neglect the adlayer interactions and in this way chemical diffusion of each species is influenced in a complicated way by the presence of coadsorbed species. It has been recognized by Evans (Tammaro and Evans, 1998) that a more complete description must include a tensorial coupling between diffusive fluxes and coverage gradients of the different adspecies and a coverage dependence of the diffusion coefficients. Such a treatment is beyond the scope of the present work and we have chosen instead to consider an Arrhenius form for diffusion $D = D_0 e^{-E_a/RT}$ with $D_0 = 10^{-7}$ m^2/s, $E_a = 7$ kcal/mol (Zhdanov, 1999).

In this section we restrict ourselves with solving the problem on a line. This is equivalent to consider that adsorbed NO only diffuses in the x-direction. In the next section we will consider the two-dimensional problem allowing then the possibility of an anisotropy in diffusion. The equations describing the system are then

$$\frac{\partial \theta_{NO}}{\partial t} = f(\theta_{NO}, \theta_i \ldots) + D_{eff} \frac{\partial^2 \theta_{NO}}{\partial x^2}, \quad (7)$$

$$\frac{d\theta_i}{dt} = f(\theta_{NO}, \ldots, \theta_i), \quad (8)$$

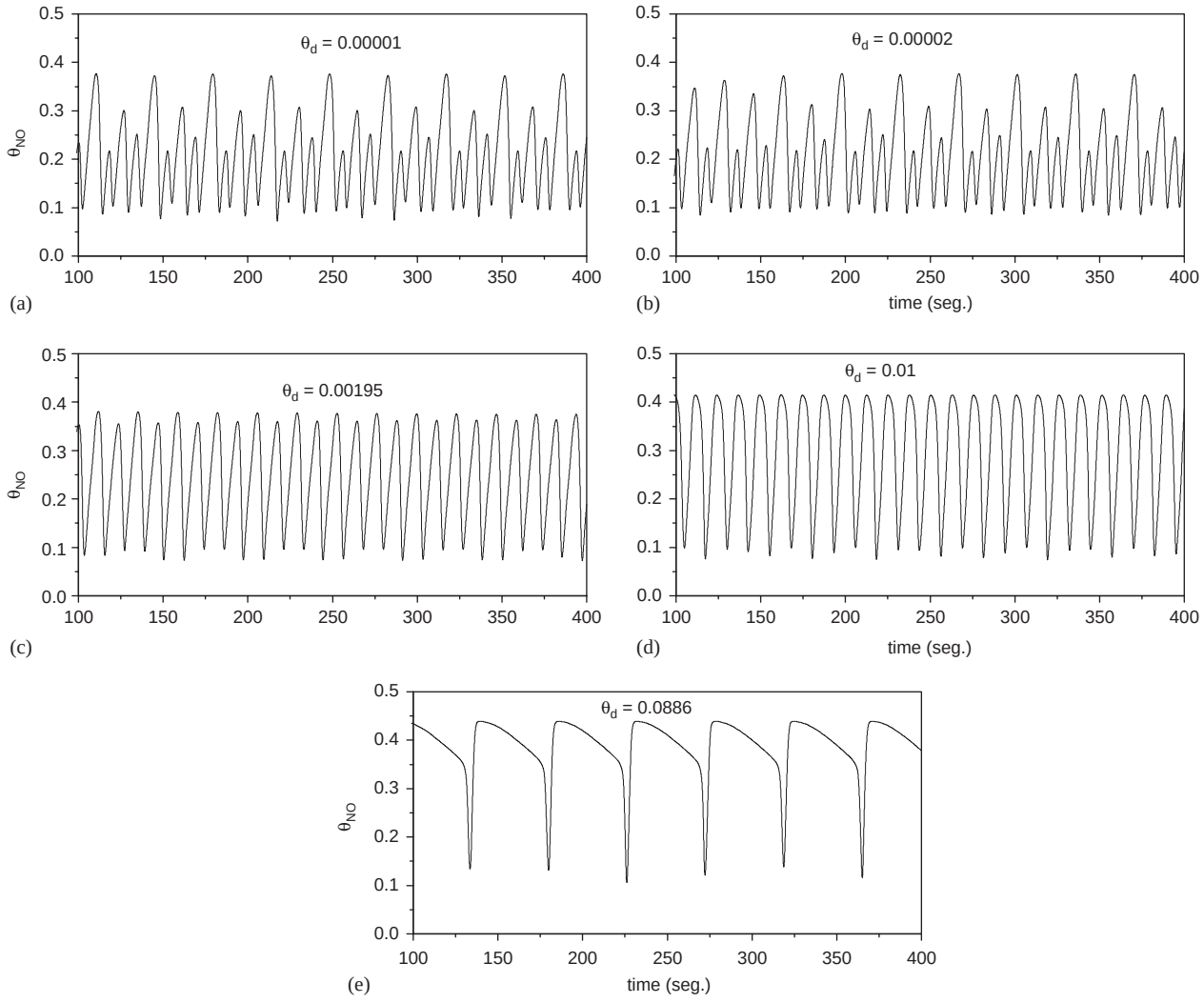

Fig. 4. Effect of increasing the fraction of impurities: (a) period-8; (b) period-4; (c) period-2; (d) period-1; (e) lenghten of period-1.

$i = \mathrm{H, N, O, NH, NH_3}$ subject to the following boundary conditions (flux of NO at the boundaries is 0):

$$t = 0, \quad \theta_{NO} = \theta_{NO_0}, \tag{9a}$$

$$x = 0, \quad \frac{d\theta_{NO}}{dt} = 0, \tag{9b}$$

$$x = L, \quad \frac{d\theta_{NO}}{dt} = 0, \tag{9c}$$

where L is the length of the ribbon or line.

As can be noted only Eq. (1) of the original model has been modified. The model consist now of one PDE coupled with 5 ODE. To solve them we used the method of lines in which one discretizes the diffusion term (we divide the space into cells of length δx) and solve the ODE across a whole line in space at each time step (see the appendix). The following remarks are noticeable:

(i) Calculations are highly sensitive to $D/\delta x$ and small changes make die the oscillations.

(ii) The period of oscillations change slightly with respect to the mean field results (see Table 2).

Again we find the period-doubling route to chaos as p is decreased for $\theta_{NO,prom}$, that is, the mean value of θ_{NO} taken over all the cells. The time series are similar to those shown in Fig. 2 and we observe P1, P2, P4, P8 and chaos. We have also calculated the corresponding power spectrum for each oscillatory record obtained by Fourier transforming the time series. At first, for example $p = 2.58$ a single peak with its harmonics is exhibited. As p is varied the period changes and more contributions in the power spectrum appear and finally for $p = 2.512$ the peaks are immersed in a broad-band structure, characteristic of aperiodic oscillations. We present here only the next-maximum map (Fig. 5) for the time series. The next-maximum map shows the accumulation of points corresponding to periods-1 to 8 and the chaotic attractor shows the characteristic single humped shape.

Fig. 6 shows the temporal behavior of θ_{NO}. Because this is a one-dimensional treatment the picture shows the

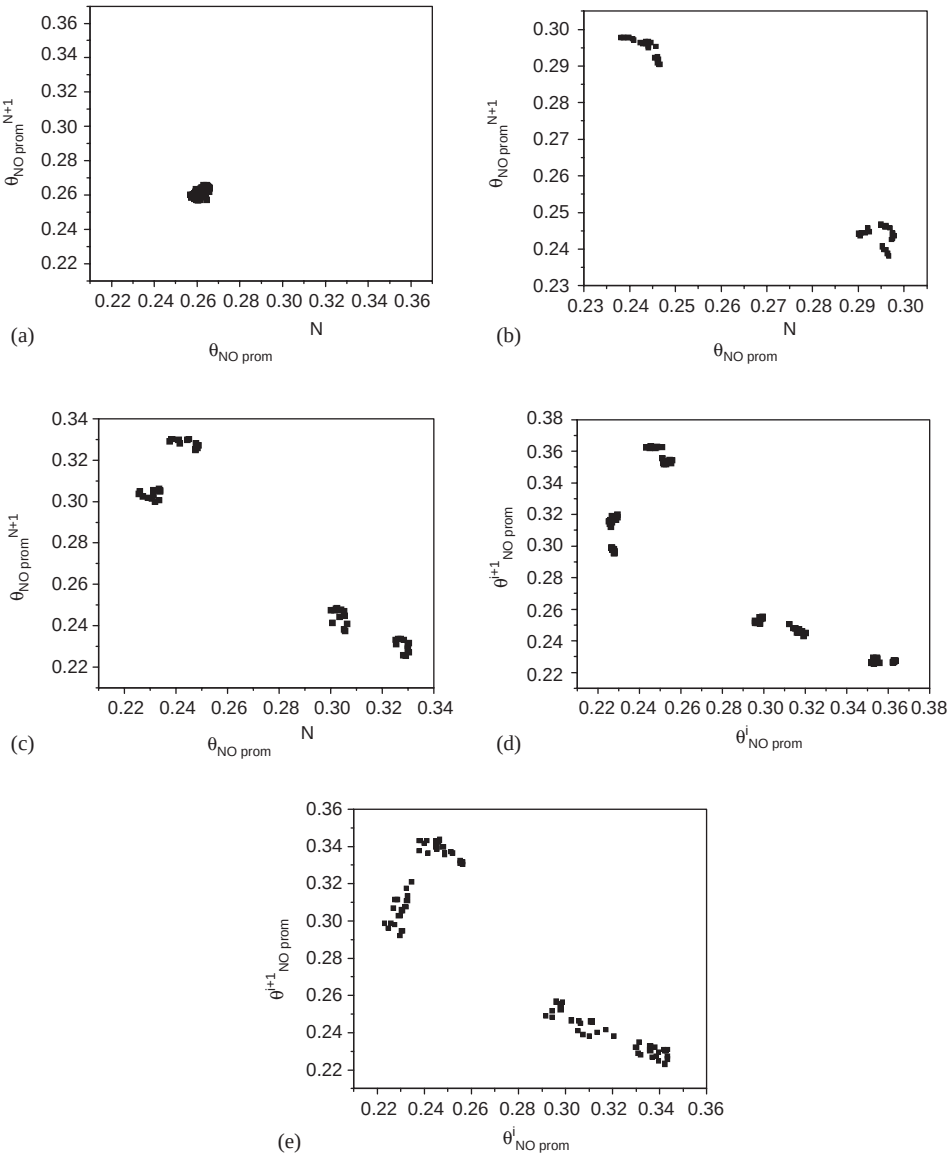

Fig. 5. Next-maximum map for the one-dimensional problem of diffusion: (a) period-1; (b) period-2; (c) period-4; (d) period-8; (e) chaos.

periodic behavior of a ribbon of a crystal divided in cells. Fig. 6a–c corresponds to P1,P2 and chaotic oscillations, respectively. Fig. 6d–f show the corresponding (top view) projections. As can be seen regular equally spaced maximum NO coverages (light gray) are formed across the crystal (Fig. 6d) as time goes on (P1). By changing p the system evolves to P2 oscillations and this changes the spacing between the adlayers (Fig. 6e) and for the chaotic state (Fig. 6f) there is no regularity between these layers.

3.2. Two-dimensions: effect of diffusivity

We consider now the two-dimensional case where again only NO diffusion is important. However we consider the possibility of an anisotry of the crystal, that is $D_{\mathrm{eff},x} \neq De_{\mathrm{eff},y}$. The equations must be modified in order to include the NO dependency on x and y. Eq. (7) is modified then to

$$\frac{\partial\theta_{\mathrm{NO}}}{\partial t} = f(\theta_{\mathrm{NO}}, \theta_i \ldots) + D_{\mathrm{eff},x}\frac{\partial^2\theta_{\mathrm{NO}}}{\partial x^2} + D_{\mathrm{eff},y}\frac{\partial^2\theta_{\mathrm{NO}}}{\partial y^2} \tag{10}$$

the rest of Eqs. (8), (9), are the same. To perform the calculations we consider a square lattice corresponding to a 0.05×0.05 mm crystal. We consider here a lattice divided into 10×10 cells. Besides the governing parameter p we consider now the effect of the anisotropy in diffusivity through the relation $D = D_{\mathrm{eff},y}/D_{\mathrm{eff},x}$. We consider first the case $D = 1$ and vary the parameter p. In order to compare with the 1-dim case we take the same values as before. Again double period transitions

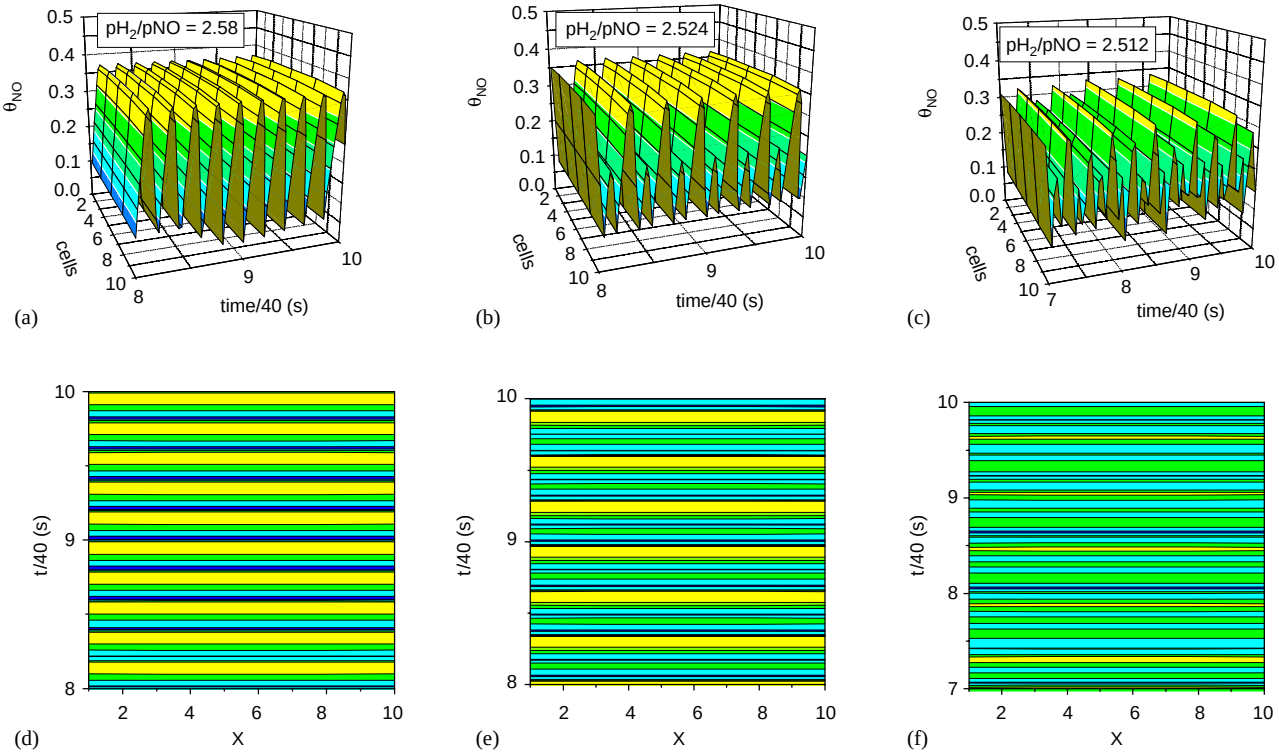

Fig. 6. Spatial behaviour of the one-dimensional problem (a ribbon of crystal divided in cells). (a–c) correspond to P1,P2 and chaotic oscillations, respectively. (d–f) show the corresponding projections (top view) showing the regular spacing in the periodic cases.

and chaos are obtained as p is varied but the numerical values are slightly changed (see Table 2). For example for $p = 2.58$ a P1 attractor is obtained but for $p = 2.518$ a P2 attractor is obtained instead of the P4 as was the case before. For $p = 2.50$ P8 oscillations are obtained instead of the chaotic oscillations as was the case before. If D is now changed small variations are also obtained. For a large value of D the results are very similar with the 1-dim case. This is expected as large values of D means a preferential diffusion in one direction. In fact, for such value as $D = 3.85$ the numerical values obtained for the transitions between the different periods are almost identical as the 1-dim case. We note that this value of the anisotry $D \sim 4$ has been also used for example in modeling anisotropic chemical wave patterns in the NO + H_2 reaction on a Rh(110) surface by Makeev et al. (2001). They used the diffusion coefficients $H[1\bar{1}0] - \text{dir} \sim 4 \times 10^{-9}\ m^2/s$ and $H[001] - \text{dir} \sim 10^{-9}\ m^2/s$. They have also considered the diffusion coefficient of $O[1\bar{1}0] - \text{dir} \sim 1.75 \times 10^{-15}\ m^2/s$ and $O[001] - \text{dir} \sim 4 \times O[1\bar{1}0]$.

In conclusion, if there is any crystal anisotropy, as described by D, the oscillatory region is shifted. In this way D could be interpreted as a new control parameter (as was the case for the impurity fraction), at least theoretically, to obtain the different transitions between oscillatory states.

3.3. Two-dimensions: influence of defects

As has been shown before, considering a homogeneous medium leads to the case of spatially uniform oscillations. In a realistic system, however the properties of the medium will not be spatially uniform, but defects will be present. One can expect that defects will make synchronization more difficult. We analyze in this part what is the effect in the global coupling as the number of defects is continuously increased.

To this end the surface nonuniformity is modeled by assuming different sticking coefficient of NO on the surface of the catalyst caused by the large sensitivity of the adsorption rate on surface dislocations. This for example has been considered by Kurtanjek and Froment (1991) in their investigation of oscillating oxidation of CO on Pt. In our simulations the sticking coefficients at some sites across the crystal have been taken arbitrarily 15% larger than the original values (Kurtanjek and Froment, 1991). Fig. 7 shows the effect of putting 2,5,12 and 32 defects symmetrically as is shown in the left part of the figure. The initial condition corresponds to a P8 attractor, that is, in the absence of any defects the final attractor would develop an 8-period orbit. We see that increasing the number of defects turns on the oscillations from P8 to P4 (Fig. 7a) to P2 (Fig. 7b and c) and with 32 defects to P1 (Fig. 7e).

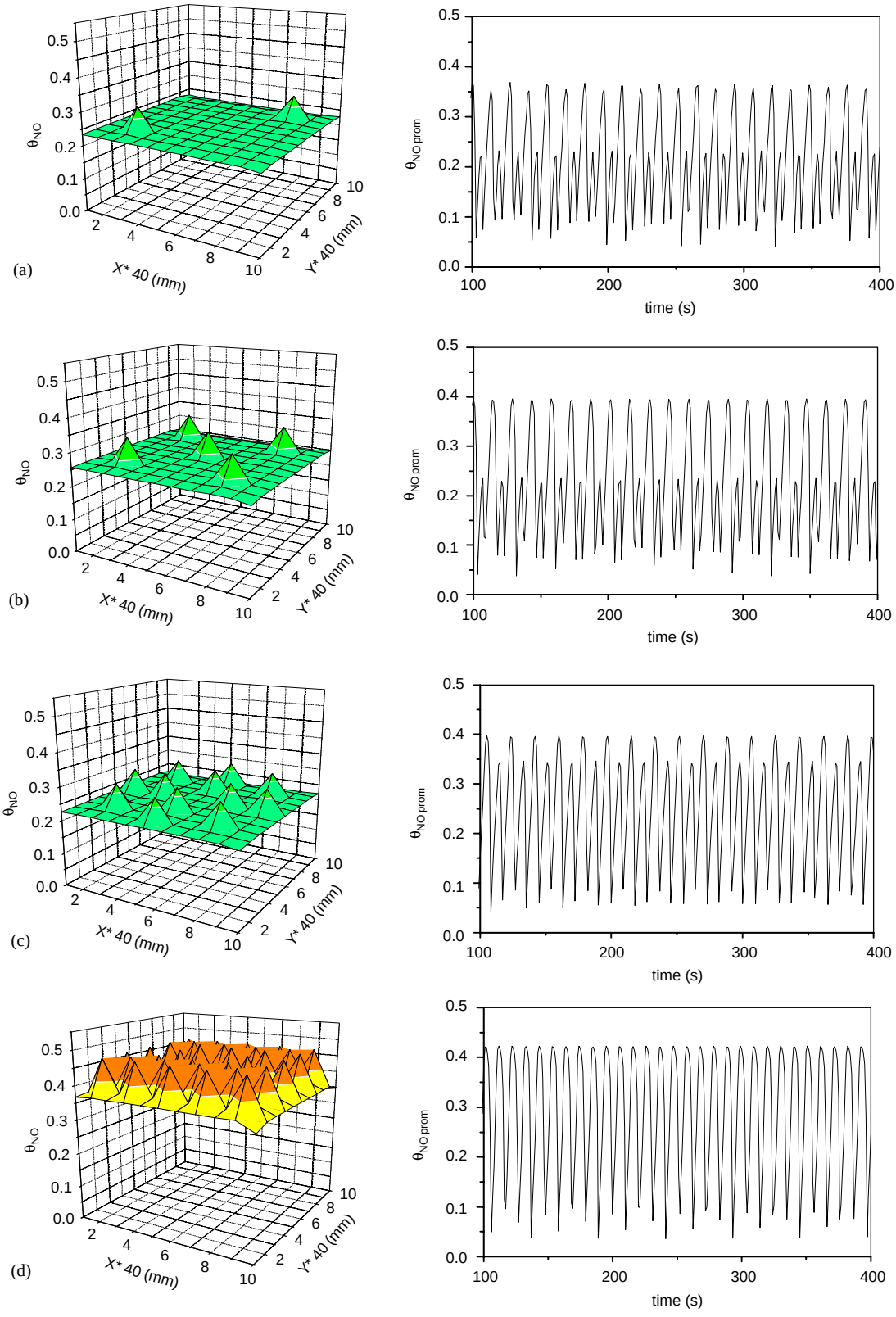

Fig. 7. Effect of increasing the number of defects in a square lattice: (a) two-defects and period-8; (b) five defects and period-2; (c) 12 defects and period-2. 32 defects and period-1. Explanation in the text.

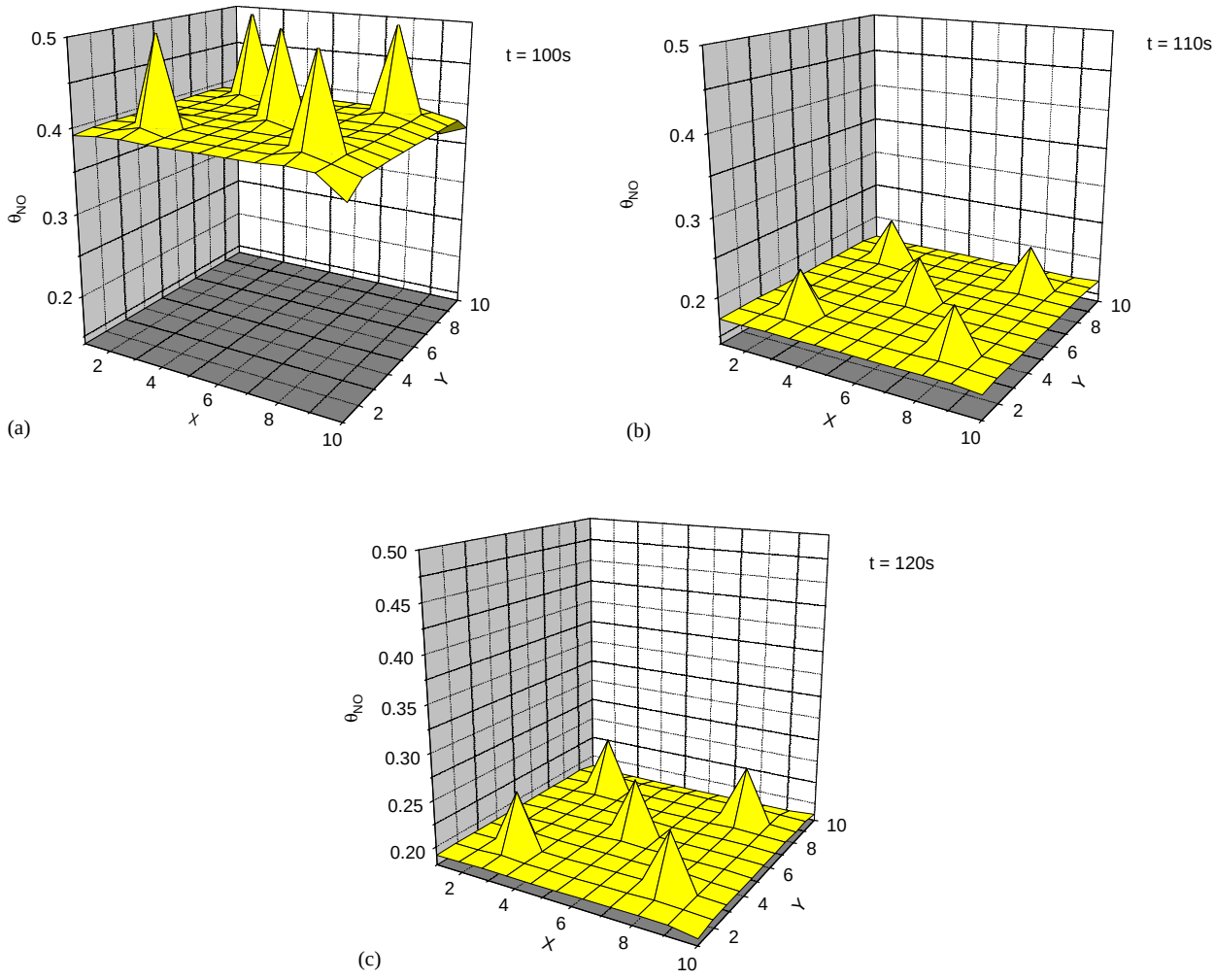

Fig. 8. Variation in time of NO coverage: (a) at $t = 100$ s; (b) at $t = 110$ s; (c) at $t = 120$ s.

The left column of Fig. 7 shows θ_{NO} at $t = 10$ s from the beginning of the simulation and what is observed as time goes on is that on the sites where defects are localized the θ_{NO} peaks grow and decrease oscillating in time. This is shown more explicitly in Fig. 8 where the three-dimensional representations for the five defects case shows θ_{NO} for times $t = 100$ s (a), $t = 110$ s (b) and $t = 120$ s (c). We have checked that placing randomly the defects do not change appreciably the oscillatory behaviour.

Resuming, the mean value oscillates in time and locally (θ_{NO} around the defects) also oscillates accordingly.

4. Monte Carlo simulations

Usually, catalytic reactions have been intensively studied by the use of mean-field modeling through ordinary differential equations as we did in the preceding sections. Such type of approach naturally involves a coarse grained description, and spatial fluctuations that lie below the typical length scale of the coarse graining (about 1 nm) are entirely neglected. MF methods consider average environments of reactants and adsorption sites ignoring stochastic fluctuations and correlations. Some of these limitations can be partially overcome by the use of computer simulations (Monte Carlo, Cellular Automata) where local environments are explicitly taken into account. These simulations have witnessed a great success since the pioneering work of Ziff et al. (1986) on an irreversible monomer–dimer reaction, which mimics in a simple way the CO oxidation on a metal surface. More refined simulations have been used to describe the surface-catalyzed CO oxidation via the Langmuir–Hinshelwood kinetics incorporing adsorbate-induced surface reconstruction (Wu and Kapral, 1992; Danielak et al., 1996; Zhadonv, 1999). They were successful in reproducing the evolution of reactant coverages and reaction rates during oscillations.

It is important to point out that the MC time is defined in these simulations via the adsorption–desorption–reactions surface restructuring events (MC time steps)

and is only roughly proportional to the actual time. Another limitation is imposed by the size of the lattices used to mimic the surface. But even with these shortcomings MC simulations is a powerful tool which contributes to the understanding of the complex behaviour of catalytic systems.

The Monte Carlo algorithm used in this work can be summarized as follows:

The surface of the catalyst is considered to be a two-dimensional lattice of active sites. The surface contains $N = 300 \times 300$ sites with periodic boundary conditions, each site surrounded by eight adjacent sites (this is the so-called Moore neighborhood consisting of the eight nearest and next-nearest neighbors). The dynamics takes place on two regular two-dimensional lattices: one of them, *Ls*, is used to represent the different phases of the substrate. Each site is assigned 0 if it is in the hex configuration and 1 if it is in the 1×1. Adsorption, desorption and migration take place in the other lattice, *La*, which contains exactly the same number of sites or nodes. On this lattice the nodes can have the following values: 0 (empty site), 1(site occupied by NO), 2 (site occupied by H) or 3 (site with adsorbed oxygen). Adsorbed species at node r can react with particles on neighboring sites $r \in N(r)$, with $N(r)$, the Moore neighborhood defined above.

In general, one would need to take into account all the steps *R*1–*R*18 but in practice the reaction can be reduced: at relatively high temperatures (high window) the rate of $NH_3(g)$ formation is lower than that of N_2 desorption (consequently, NH is neither appreciable). Then, for the purposes of our simulation we consider the following simplified mechanism for the $NO + H_2$ reaction:

$$NO + * \underset{k_2}{\overset{k_1}{\rightleftharpoons}} NO_{ads}, \qquad \text{(M1–M2)}$$

$$H_2 + * \underset{k_4}{\overset{k_3}{\rightleftharpoons}} 2H_{ads}, \qquad \text{(M3–M4)}$$

$$NO_{ads} \overset{k_5}{\longrightarrow} N_{ads} + O_{ads}, \qquad \text{(M5)}$$

$$2N_{ads} \overset{k_N}{\longrightarrow} N_2 + 2*, \qquad \text{(M6)}$$

$$2H_{ads} + O_{ads} \overset{k_r}{\longrightarrow} H_2O(g) + 2*, \qquad \text{(M5)}$$

where * represents an empty active site on the catalytic surface. In practice, Eq. (M6) is not considered, because it is a very fast process. This means that nitrogen atoms are essentially removed immediately after the adsorption of NO takes place. The numerical implementation of these reactions is essentially similarly to that presented in earlier works (Danielak et al., 1996; Chávez et al., 2000), for the $CO + O_2$ system.

Diffusion of the NO species will be considered through random jumps of the adsorbed species at node **r** to one of the empty nodes in the neighborhood. In this way we have now five possible processes (adsorption, desorption, dissociation, chemical reaction, diffusion) and the set of rate constants is denoted by $K^I = (K_1^I, \ldots, K_5^I)$, where the superscript I denotes the constants for the hex phase. A similar notation K^{II} is followed for the 1×1 phase. (In general the reaction rates may be different for the two surface phases). In particular we will denote K_H, K_{NO} the adsorption constants for H and NO, respectively. The rates of NO and H_2 adsorption are considered to be proportional to p_{NO} and p_{H_2}, respectively, and the ratio $p = K_H/K_{NO}$ is thus only proportional to the ratio of Section 21. Finally, all the rates are slow compared to NO diffusion.

The set of reaction rates defines the probability $p_i = K_i / \sum K_i$, that the ith process is carried out at a lattice point. Each time step consists of N applications of the composition of the following operations:

1. A node r is chosen at random.
2. A process i is chosen with probability p_i.
3. In the case of processes involving simultaneously two adjacent nodes (hydrogen adsorption/desorption, chemical reaction, surface diffusion), a second node is randomly selected from $N(r)$.
4. If the chosen process is sterically possible in the selected site, it is carried out and values of the sites are updated. If it is not possible, the trial is disregarded. In any case the sequence is started over from step 1 above. If the phase transformation step is selected then a substrate phase transformation is attempted by the following mechanism. Let us denote $n_{NO}(r)$ the number of molecules of NO adsorbed at the neighborhood of node r on lattice *La*, and $n(1 \times 1)(r)$ the number of sites of the neighborhood of node r on lattice *Ls* which have surface structure (1×1). We distinguish four basic steps:

   (a) (1×1) domain formation mechanism. If all nodes in $N(r)$ on *La* are in the hex phase and $n_{NO}(r) = 9$ (the neighborhood is covered by NO), then node r is changed to (1×1).
   (b) (1×1) domain growth mechanism. If node r is in the hex phase and $n_{NO}(r) > r_{max}$, then node r is changed to (1×1) with probability $F(n(1 \times 1)) = n(1 \times 1)/9$. Here, r_{max} is a parameter which represents some lower fixed fractional coverage necessary for (1×1) domain growth.
   (c) hex domain formation. If all nodes in $N(r)$ on La are in the (1×1) phase and $n_{NO}(r) = 0$, then node r is changed to hex.
   (d) hex domain growth. If node r is in the (1×1) phase and $n_{NO}(r) < r_{min}$, then node r is changed to hex

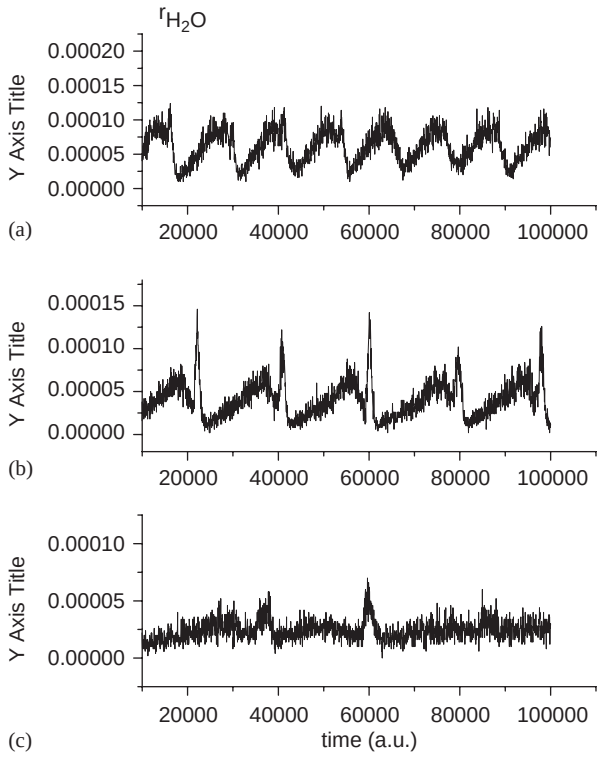

Fig. 9. The production rate r_{H_2O} versus time (simulation steps) for three different values of $p = K_{H_2}/K_{NO}$. The simulations show the change in period one (a) $p = 0.003$ to two (b) $p = 0.002$. The oscillations become irregular and chaotic as p is further decreased to (c) $p = 0.0008$.

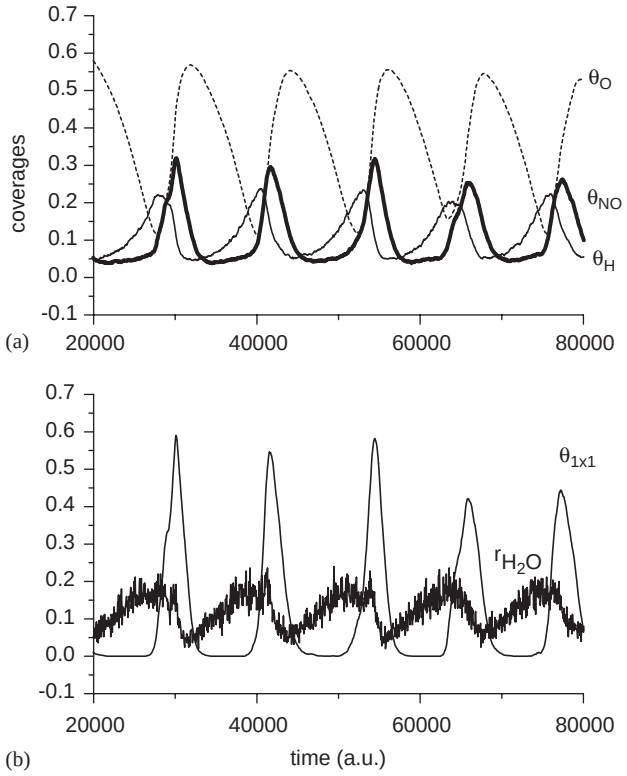

Fig. 10. Oscillatory time series for $p = 0.003$: (a) bold line for NO coverage, thin line for H and dash line for O; (b) thin line for $\theta_{1\times1}$ and thick line for r_{H_2O} production (1000 times increased).

with probability $F(n(1\times1)) = 1 - n(1\times1)/9$. Here, r_{max} is a parameter which represents some upper fixed fractional coverage necessary for hex domain growth.

The phase transformation steps described in this way mimic the real process (Danielak et al., 1996; Chávez et al., 2000) and are consistent with the Imbihl description of SPT, that is, with what is observed experimentally (domain nucleation and growth). In our simulations we use K_{NO} as a control parameter and maintain constant the other K_i. The results of the simulations are summarized in Figs. 9–11.

Fig. 9 shows the oscillations in r_{H_2O}, the rate of H_2O production for three different values of $p = K_{H_2}/K_{NO}$.

The figure shows single period oscillations (Fig. 9a) and when p is decreased a period doubling is observed (Fig. 9b). If p is further decreased the oscillatory behavior is lost and we obtain irregular or chaotic oscillations (Fig. 9c). The simulations do not show any tendencies for more than two periods.

Fig. 10a shows θ_{NO}, θ_O and θ_H. The first two are almost in phase whereas θ_H is out of phase. This agrees with the results of Fig. 1b. Fig. 10b shows the $\theta_{1\times1}$ coverage and the H_2O production (multiplied by 1000). We see in this figure that the maxima in $\theta_{1\times1}$ correlate roughly with the minima in the r_{H_2O} peaks, that is, the maxima in hex reconstruction correlates with maxima in H_2O production. To our knowledge there is not detailed experimental data for the NO + H_2 reaction to verify this, but this fact has been well established for the similar reaction NO + CO/Pt(100): the maximum in catalytic activity correlates with the maximum in hex reconstruction (Veser and Imbihl, 1994).

In Fig. 11a–f we show snapshots of both the species and substrate for three points of the times series shown in Fig. 10b corresponding to times $t = 50\,000$(a.u.) (this the maximum in r_{H_2O} production) and at intervals $\Delta t = 500$ (a.u.) latter. We can see how the substrate evolves by nucleation and growth of the 1×1 phase (black region in Fig. 11b,d and f). The $\theta_{1\times1}$ fractions are successively (b) 0.19, (d) 0.41, (f) 0.62. The formation of islands is clearly shown in Fig. 11d.

At the left column (Fig. 12a,c and e) the coverages are (θ_{NO}=0.13, θ_H=0.22, θ_O=0.25), (θ_{NO}=0.22, θ_H=0.22, θ_O= 0.27), ($\theta_{NO} = 0.32, \theta_H = 0.16, \theta_O = 0.36$).

At first (Fig. 11a) there is an almost random distribution of NO(dark gray), H(light gray) and O(black). This corresponds to the maximum in H_2O production as the trials O + 2H in the simulation occurred more frequently. As time goes on strong clustering occurs (Fig. 11c and e). Fig. 11f

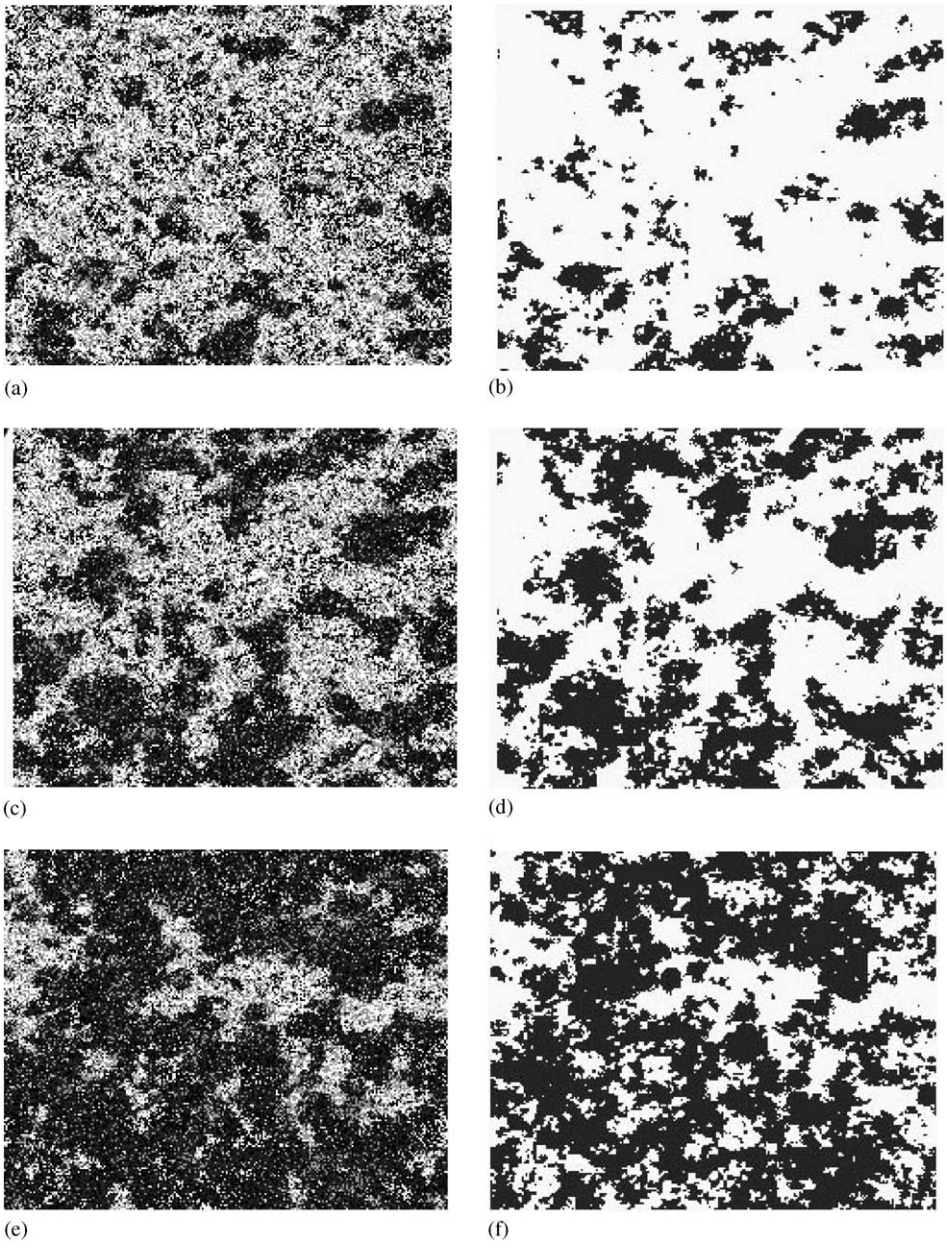

Fig. 11. (a–f). The temporal evolution of the species (left) and substrate (right) corresponding to the time series shown in Fig. 10a. The initial time is $t = 12\,500$ and increments of $\Delta t = 500$. For the species lattice, NO is shown in dark gray, O in black and H in light gray. For the substrate lattice, hex is in white and 1×1 in black.

corresponds to a maximum in $\theta_{1\times1}$ reconstruction, then this fraction decreases and the lattice returns at the end of the cycle.

5. Conclusions

Within the mathematical MF model proposed by Makeev and Nieuwenhuys (1998a, b) for the $NO + H_2$ reaction on Pt(100)it has been shown that decreasing the controlling parameter p (ratio of partial pressures) causes the system to undergo transitions from simple oscillations to chaos through period-doubling bifurcations. Near the critical point the dependence of the amplitude of oscillations on the partial pressures ratio p is shown to be very close to that predicted for the Hopf supercritical bifurcation. The inclusion of non-uniformities, in the form of blocking sites or defects changes the oscillatory periods. The effect of increasing continuously the number of defects is to decrease the period of oscillations. So we can suggest the experimentalist that a way to change the oscillatory behavior of their samples is to create defects

(by annealing, for example). We have extended also the model to consider a two dimensional lattice and show that changes in the diffusivity in the x and y directions also changes the oscillation periods. So a bifurcation diagram must consider besides the partial pressure ratio p, the diffusivity D and the fraction of blocking sites θ_d or defects.

We have presented also Monte Carlo simulations of the oscillatory NO–H_2 reaction on Pt(100). In this simulations our results allow to correlate adsorption coverages and hex fraction with H_2O production. We also observe island formation during the oscillatory cycle which is in agreement with the experiments. The simulations complements the mean field approach by allowing the study of the fluctuations of the surface coverages.

With the mechanism displayed in Eqs. (M1–M6) and SPT we obtain oscillations in $\theta_{NO}, \theta_H, \theta_O$ and a period doubling for r_{H_2O}. But this mechanism alone is not able to show more than 2-period oscillations. In fact the studies by Lombardo et al. (1993), Gruyters et al. (1996) which includes SPT do not show the appearance of chaos. The appearance of period doubling mechanism was shown to appeared via the MF equations (Section 2.1) (without SPT) due to the highly nonlinear character of the ODE Eqs. (1)–(6) and the strong interactions. It is very difficult to implement such interactions at the level of Monte Carlo rules. In conclusion, Monte Carlo simulations who take into consideration realistic mechanism of the NO+H_2/Pt(100) reaction to describe transition to chaos via period doubling are still lacking.

Notation

D_{eff}	effective diffusion coefficient of chemisorbed NO, $m^2\ s^{-1}$.
D	ratio of diffusion coefficients of NO in directions x and y.
I_α	lateral interactions
k_i	reaction rates
L	characteristic length of catalyst
p_{NO}	NO partial pressure, bar
p_{H_2}	H_2 partial pressure, bar
R_i	rates of elementary reaction steps
S_i	sticking probabilities, $i = NO, H_2$
t	time, s
T	catalyst temperature, K

Greek letters

ε_{ap}	parameters of lateral interactions
θ_i	fractional coverage of chemisorbed species, $i = NO, H, N, O, NH, NH_3$
θ_*	fraction of free adsorption sites θ_d fraction of blocked sites (impurities)

Acknowledgements

The funding provided by CONACYT through grant 32228-E is gratefully acknowledged.

Appendix

To solve the PDE (Eqs. (7–10)) we have used the method of lines, in which one discretizes the diffusion term and then solve the ODE problem across a whole line in space at each time step. In this way the equations to solve in the two-dimensional case are:

$$\frac{d\theta_{NO}}{dt} = f(\theta_{NO}, \theta_i \ldots) + D_{eff,x}\frac{\theta_{NO}^{k-1} - 2\theta_{NO}^{k} + \theta_{NO}^{k+1}}{\delta x} + D_{eff,y}\frac{\theta_{NO}^{(k-1)-M} - 2\theta_{NO}^{k} + \theta_{NO}^{(k+1)+M}}{\delta y},$$

$M \times M$ is the number of lattice sites
$N = M \times M + 5$,
$k = 1, 2, \ldots, N - 5$,

$$\frac{d\theta_i}{dt} = f(\theta_{NO}, \ldots, \theta_i),$$

$i = H, N, O, NH, NH_3$ subject to the following boundary conditions:

$$t = 0, \quad \theta_{NO} = \theta_{NO_0},$$

$$x = 0, \quad \frac{d\theta_{NO}^{1}}{dx} = 0, \quad \frac{d\theta_{NO}^{1}}{dy} = 0,$$

$$x = L, \quad \frac{d\theta_{NO}^{M}}{dx} = 0, \quad \frac{d\theta_{NO}^{M}}{dy} = 0.$$

Finally to solve these equations Gear's method has been employed with a high quality solver (IMSL).

References

Asakura, K., Lauterbach, J., Rotermund, H.H., Ertl, G., 1994. Modification of spatiotemporal pattern formation in an excitable medium by continuous variation of its intrinsic parameters: CO oxidation on Pt(100). Physical Review B 50, 8043–8046.

Asakura, K., Lauterbach, J., Rotermund, H.H., Ertl, G., 1997. Spatio-temporal pattern formation during catalytic CO oxidation on a Pt(100) surface modified with submonolayers of Au. Surface Science 374, 125–141.

Chávez, F., Vicente, L., Perera, A., 2000. Kinetic oscillations in the catalytic CO oxidation on Pt(100) with adsorbed impurities. Journal of Chemical Physics 113, 10353–10360.

Cobden, P.D., Siera, J., Nieuwenhuys, B.E., 1992. Oscillatory reduction of nitric oxide with hydrogen over Pt(100). Journal of Vacuum Science and Technology A10, 2487–2494.

Danielak, A., Perera, A., Moreau, M., Kapral, R., 1996. Surface structure and catalytic CO oxidation oscillations. Physica A 229, 428–443.

Dixon-Warren, St.J., Pasteur, A.T., King, D.A., 1995. Nonlinear effects in the hydrogen/deuterium catalytic exchange reaction over Pt(100). Journal of Chemical Physics 103, 2261–2271.

Egelhoff Jr., W.C., 1982. In: King, D.A., Woodruff, D.P. (Eds.), The Chemical Physics of Solid Surfaces and Heterogeneous Catalysis, Vol. 4, Fundamental Studies of Heterogeneous Catalysis. Elsevier, Amsterdam.

Fink, Th., Dath, J.-P., Basset, M.R., Imbihl, R., Ertl, G., 1991a. The mechanism of the "explosive" NO + CO reaction on Pt(100): experiments and mathematical modeling. Surface Science 245, 96–110.

Fink, Th., Dath, J.-P., Imbihl, R., Ertl, G., 1991b. Kinetic oscillation in the NO + CO reaction on Pt(100): experiments and mathematical modeling. Journal of Chemical Physics 95, 2109–2126.

Gear, C.W., 1971. Numerical Initial Value Problems in Ordinary Differential Equations. Prentice-Hall, Englewood Cliffs, NJ.

Gruyters, M., Pasteur, A.T., King, D.A., 1996. Simulation of oscillatory behaviour in the reduction of NO by hydrogen on Pt(100): the role of non-linear restructuring. Journal of the Chemical Society Faraday Transactions 92, 2941–2949.

Imbihl, R., 1993. Oscillatory reactions on single crystals surfaces. Progress in Surface Science 44, 185–343.

Imbihl, R., Ertl, G., 1995. Oscillatory kinetics in heterogeneous catalysts. Chemical Reviews 95, 697–733.

Imbihl, R., Cox, M.P., Ertl, G., Müller, H., Brenig, W., 1985. Kinetic oscillations in the catalytic CO oxidation on Pt(100): theory. Journal of Chemical Physics 83, 1578–1587.

Imbihl, R., Cox, M.P., Ertl, G., 1986. Kinetic oscillations in the catalytic CO oxidation on Pt(100): experiments. Journal of Chemical Physics 84, 3519–3534.

Kurtanjek, Ž., Froment, G.F., 1991. An investigation of surface phenomena associated with oscillating oxidation of CO on Pt. Chemical Engineering Science 46, 3189–3201.

Lesley, M.W., Schmidt, L.D., 1985. The NO + CO reaction on Pt(100). Surface Science 215–240.

Lombardo, S.J., Fink, T., Imbihl, R., 1993. Simulations of the $NO + NH_3$ and $NO + H_2$ reactions on Pt(100): steady state and oscillatory kinetics. Journal of Chemical Physics 98, 5526–5539.

Madden, H.H., Imbihl, R., 1991. Interaction of NO and H_2 with Pt(100). Applied Surface Science 48/49, 130–134.

Makeev, A.G., Nieuwenhuys, B.E., 1998a. Mathematical modeling of the NO + H_2/Pt(100) reaction: "surface explosion," kinetic oscillations, and chaos. Journal of Chemical Physics 108, 3740–3749.

Makeev, A.G., Nieuwenhuys, B.E., 1998b. Simulation of oscillatory behaviour in the $NO + H_2$ reaction on a partially reconstructed Pt(100) surface. Surface Science 418, 432–440.

Makeev, A., Hinz, M., Imbihl, R., 2001. Modeling anisotropic chemical wave patterns in the NO + H_2 reaction on a Rh(110) surface. Journal of Chemical Physics 114, 9083–9098.

Peeters, P., Baras, F., Nicolis, G., 1990. Sensitivity of the chlorite-thiosulfate system: a stochastic approach. Journal of Chemical Physics 93, 7321–7328.

Scott, S.K., 1991. Chemical Chaos. Clarendon Press, Oxford.

Siera, J., Cobden, P., Tanaka, K., Nieuwenhuys, B., 1991. The nitric oxide-hydrogen reaction over Platinum (100): oscillatory behavior of activity and selectivity. Catalysis Letters 10, 335–342.

Slinko, M.M., Jaeger, N.I., 1994. Oscillating Heterogeneous Catalytic Systems. Elsevier, Amsterdam.

Slinko, M.M., Fink, T., Loher, T., Madden, H.H., Lombardo, S.J., Imbihl, R., Ertl, G., 1992. The $NO + H_2$ reaction on Pt(100): steady state and oscillatory kinetics. Surface Science 264, 157–170.

Tammaro, M., Evans, J.W., 1998. Reactive removal of unstable mixed NO+CO adlayers: chemical diffusion and reaction front propagation. Journal of Chemical Physics 108, 7795–7806.

Veser, G., Imbihl, R., 1994. Synchronization and spatiotemporal self-organization in the NO+CO reaction on Pt(100). II. Synchronized oscillations on the hex-substrate. Journal of Chemical Physics 100, 8492–8500.

Wu, X.G., Kapral, R., 1992. Catalytic Co oxidation on Pt surfaces: a lattice gas cellular automaton model. Physica A 188, 284–301.

Zhdanov, V.P., 1999. Surface restructuring and kinetic oscillations in heterogeneous catalytic reactions. Physical Review E 60, 7554–7557.

Zhdanov, V.P., 2002. Monte Carlo simulations of oscillations, chaos and pattern formation in heterogeneous catalytic reactions. Surface Science Reports 45, 231–326.

Ziff, R.M., Gulari, E., Barshad, Y., 1986. Kinetic phase transitions in an irreversible surface reaction model. Physical Review Letters 56, 2553–2556.